A critique of the THUMS lower limb model for pedestrian impact applications

Thomas Cloake[1], Christophe Bastien[1], Joseph Hardwicke[2], Demetrios Venetsanos[1], Clive Neal-Sturgess[1]

[1]Institue for Future Transport and Cities, Coventry University, UK
[2]University Hospitals Coventry and Warwickshire, Coventry, UK

Abstract

The Total Human Model for Safety (THUMS) is widely used for biomechanics research and validated at the component and full-body levels. Nonetheless, some authors have reported differences in predictions between the model and real-life injuries, particularly in the lower limbs. This study aims to perform an extensive critique of the THUMS lower limb and identify areas for improvement. The THUMS model was assessed across quasi-static and dynamic validation tests to understand geometry, material properties and response to impact. The study has highlighted that the THUMS' geometry is comparable to published cadaveric data for bones and ligaments, but soft tissues (muscle, adipose and skin) and fascia have significant simplifications. The bones' material properties are evidence-based and vary appropriately according to anatomical site. Bone failure is permitted through element deletion; however, the unusually transverse fracture pattern predicted in THUMS is seldom seen in clinical practice. The simplified soft tissue model cannot fail, making it unable to replicate the extensive damage seen in high energy open fractures. Ligament injury is a frequent result of an impact to the pedestrian lower limb, often at the bone-tendon interface, yet the failure location seen in the THUMS model is mid-substance. In summary, THUMS makes an excellent attempt to model the lower limb; nonetheless, some work is still required to increase biofidelity. Improvements in soft tissue geometry and material properties and fracture pattern modelling represent apparent areas for development.

1 Background

Injuries to pedestrians remain a significant source of morbidity and mortality. There are over 20,000 pedestrian casualties per year in the UK, with one-third of these resulting in death or severe injury [1]. Lower limb injuries are sustained in up to 30% of road traffic accidents involving pedestrians [2], and they are a source of significant disability and impairment [3]. There has, therefore, been much interest in modelling lower limb injuries. Contemporary advances in computational engineering have led to sophisticated human body models that accurately predict the site and nature of injuries following impact. Numerous models are currently available, exhibiting variation in posture, anthropometry, and age. At the turn of the twenty-first century, the Total Human Model for Safety (THUMS) was pioneered by Iwamoto et al. [4]. The model was based on the anthropometry of a 50th percentile adult, using cross-sectional imaging to create a detailed mesh complete with skeleton, internal organs and soft tissue coverings. Further refinement has produced age and gender-specific models [4] and the capability to model active muscles [5]. THUMS has been extensively validated against cadaveric studies [6], showing excellent agreement with experimental injuries. Moreover, THUMS simulations have been compared with real-life accident data to show a good correlation in most body regions [7]; however, there are some reported discrepancies in lower limb injuries [8; 9]. This study aims to comprehensively review the THUMS lower limb model focusing on pedestrian impact applications and identify areas for future development.

2 Methodology

The critique was conducted by a mechanical engineer with extensive experience in automotive engineering and crash safety as well as a Trauma and Orthopaedic and Plastic and Reconstructive Surgeon, both with experience in managing lower limb trauma. THUMS AM50 version 4.02 was used as the model for evaluation, and an assessment was performed using the Oasys LS-DYNA software suite [10]. The analysis began by assessing the geometry of the model in relation to published anthropometric and cadaveric measurements. Material properties were then assessed in detail alongside a review of contemporary attempts to model biological tissues in regional and full human body models. THUMS kinematic response to impact was reviewed using the validation tests available from Toyota [11]. Specific injury patterns were then analysed, considering physical outputs from each

anatomical structure. Additionally, the authors' experience as a surgeon was used to compare model predictions to those injuries seen in clinical practice.

3 Geometry

Replication of the complex anatomy seen within the human body is essential for creating a biofidelic model. Early versions of the THUMS lower limb [6] relied upon the Viewpoint Datalabs resource to provide the geometrical average of 30 lower limb bones. Subsequent versions have utilised cross-sectional imaging in the form of computed tomography (CT) scans of a 50th centile adult to create a detailed mesh.

3.1 Bones

The THUMS model offers an accurate representation of the bony morphology of the lower limb. The major features of the lower limb long bones are present, including a complex head and neck region at the proximal femur as well as appropriately accurate femoral condyles and tibial plateau to create an anatomically accurate knee joint. The complex prismoid shape of the tibia is present and there is gentle anterior bowing of the femur and tibia. The general dimensions of the long bones within THUMS are in keeping with reference values (Figure 1).

FEMUR
THUMS length = 45.0 cm
Reference = 43.7 cm [12]

TIBIA
THUMS length = 38.5 cm
Reference = 37.9 cm [14]

FIBULA
THUMS length = 39.1 cm
Reference = 38.4 cm [13]

Fig.1: Anthropometric dimensions of lower limb long bones in THUMS model compared to reference values [12–14]

There is a gradual change in cortical thickness in an axial section from the diaphysis (thick cortical bone) to the metaphysis (thinner, predominantly cancellous bone), representing proper anatomy. (Figure 2). Accurate modelling of cortical thickness variation is also evident in cross-sections of the femur.

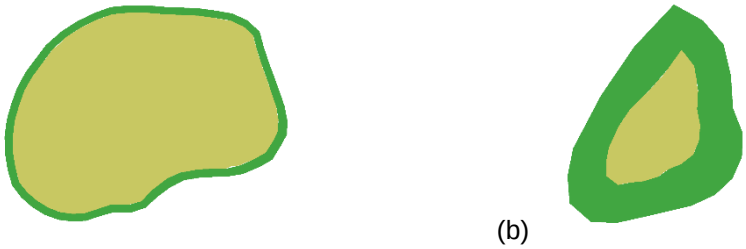

(a) (b)

Fig.2: Transverse sections of the tibia at proximal metaphysis (a) and mid-diaphysis (b). Green = cortical bone. Yellow = cancellous bone

3.2 Ligaments and tendons

The knee's four major ligaments are present within the THUMS model, namely the medial and lateral collateral ligaments alongside the anterior and posterior cruciate ligaments. The medial collateral ligament (MCL) is the most commonly injured ligament within the knee [15]. Acting to resist valgus and rotational forces, it consists of 2 distinct layers – superficial and deep [16]. The superficial MCL is the largest structure of the medial knee, originating above and behind the medial femoral condyle and

inserting at the posteromedial tibial crest [17]. The deep MCL can be thought of as a thickening of the capsule and is closely related to the medial meniscus [17]. Whilst the origin, insertion and course of the MCL in the THUMS model appears acceptable (Figure 3a), it lacks the detail of being formed of two layers and its anatomical relations. The dimensions of the MCL in the model give a length of 90.3mm and a maximal width of 18.5mm. This is roughly in agreement with cadaveric studies, with the width being comparable (11.7 mm) but the length at the lower end of measured values (94.8 mm) [18]. The lateral collateral ligament is less complex and can be considered a tubular structure that runs between the posterior, proximal lateral femoral condyle to the fibula head [19], mirrored in the THUMS model (Figure 3b). Its dimensions are 63.6 mm in length and 5.8 mm in width, reflecting reported values in the literature [20].

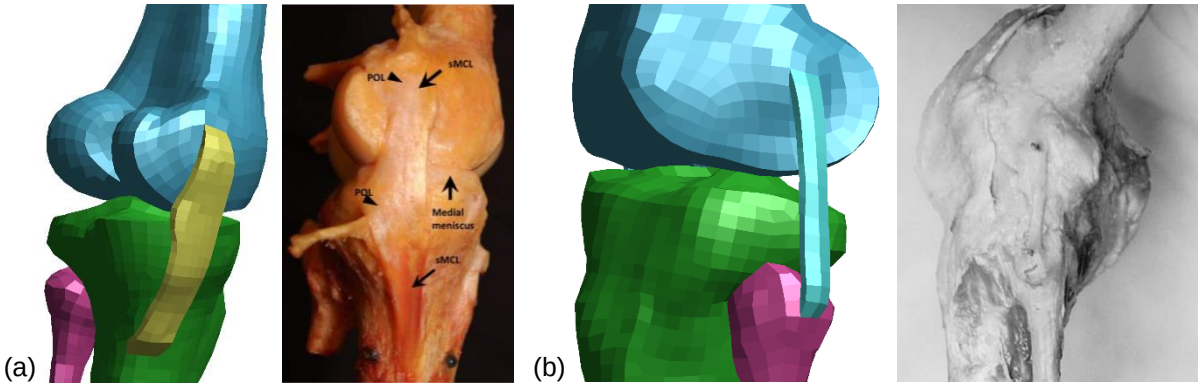

MEDIAL COLLATERAL LIGAMENT
THUMS dimensions = 90.3 mm x 18.5 mm
Reference = 94.8 mm x 17.7 mm [18]

LATERAL COLLATERAL LIGAMENT
THUMS dimensions = 63.6 mm x 5.8 mm
Reference = 66 mm x 3.4 mm [20]

Fig.3: Medial (a) and lateral (b) views of the knee demonstrating the morphology of collateral ligaments on the THUMS model and cadaveric specimens. [18; 20]

The anterior cruciate ligament (ACL) is a structure made of several tissue bundles that originate at the lateral intercondylar ridge of the femur and inserts between the intercondylar eminences of the tibia [21]. Similarly, the posterior cruciate ligament (PCL) has two bundles running from the medial femoral condyle to the posterior tibia [22]. The ACL dimensions in THUMS appear to replicate the values reported in the literature [23] (Figure 4). Interestingly, the PCL has an almost four-fold larger cross-sectional area within the model [24], hence potentially influencing its stiffness.

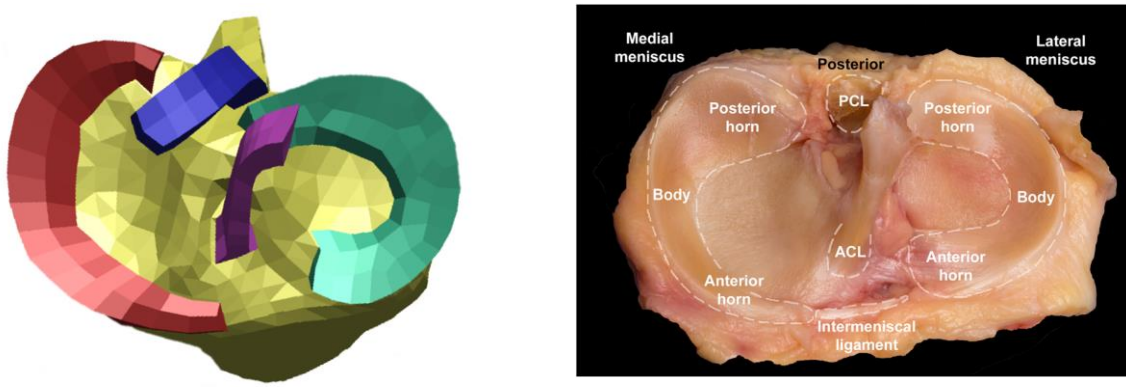

ANTERIOR CRUCIATE LIGAMENT
THUMS dimensions = 36 mm length, 31.2 mm^2 cross section
Reference = 26 – 38 mm length, 30 – 53 mm^2 cross section [23]

POSTERIOR CRUCIATE LIGAMENT
THUMS dimensions = 32 mm length, 46.8 mm^2 cross section
Reference = 32 – 38 mm length, 11 – 13 mm^2 cross section [24]

Fig.4: Caudal view of the tibial plateau demonstrating the anterior cruciate ligament (purple) and posterior cruciate ligament (blue) in THUMS and the corresponding region of a cadaveric tibia (right). (Image reproduced from [25]*)*

3.3 Soft tissues

The soft tissues (muscle, adipose, skin) comprise a significant volume of the lower leg. The THUMS model contains two distinct soft tissue layers described as ‘skin’ and ‘flesh’, with the flesh layer subdivided into rudimentary compartments. Figure 5 illustrates the difference in detail of transverse sections taken from various distances along the leg and compares these with anatomical diagrams and

transverse sections from an MRI scan. The THUMS model makes some significant simplifications in terms of soft tissue structures at all levels. Muscle compartments are present throughout; however, their size and relative proportions are not always representative. This is particularly evident at the ankle, where instead of key posterior compartment muscles (gastrocnemius and soleus), there appears to be an empty space. Moreover, the medial aspect of the tibia, which in human anatomy is covered by a thin layer of fascia beneath the skin, has an unusually thick ‚flesh' compartment (Figure 5).

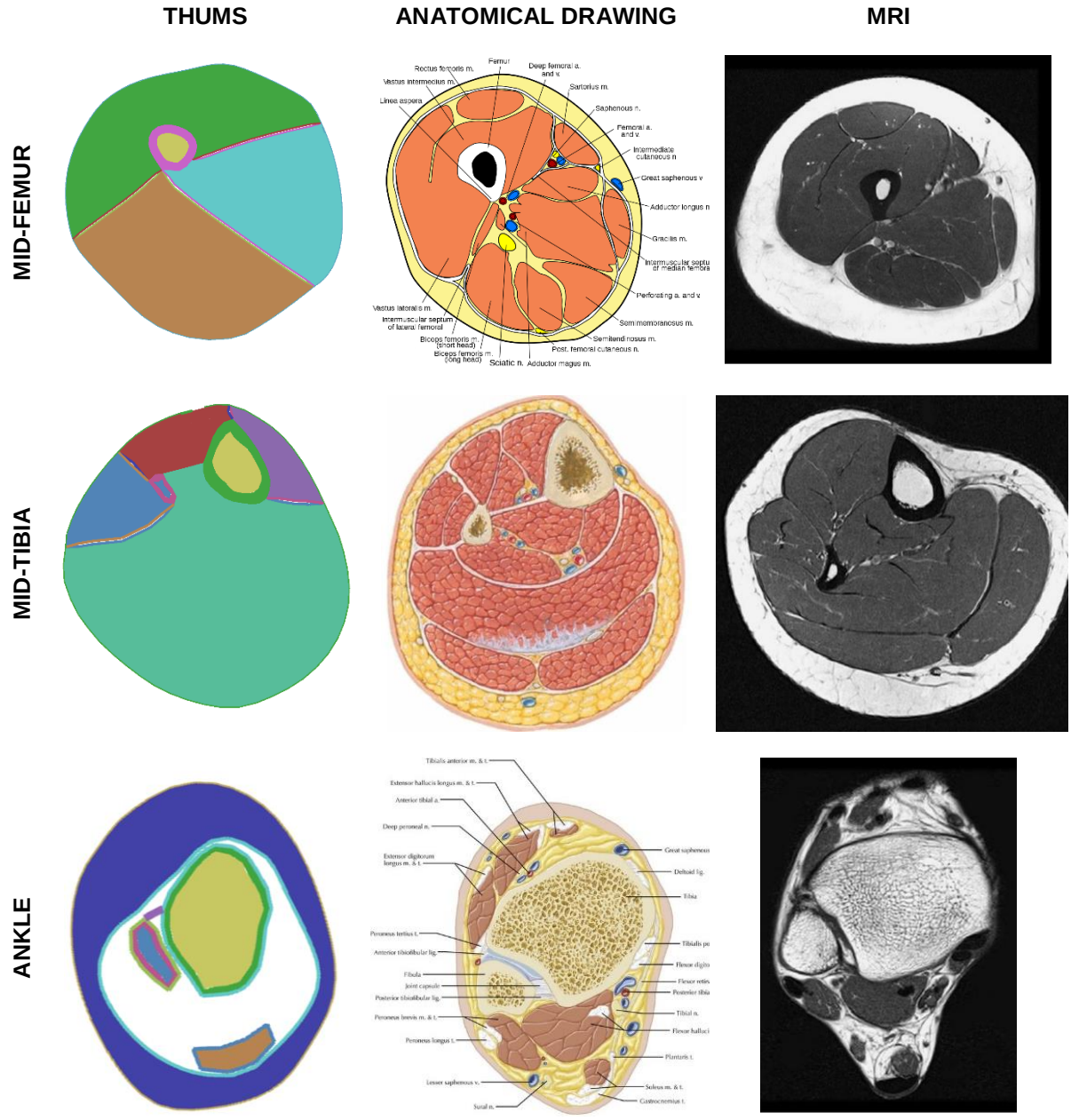

Fig.5: Axial sections taken through the leg at various anatomical levels. The left column displays cut sections from the THUMS model. The middle column shows anatomical diagrams of the corresponding sections. The right column contains magnetic resonance images (MRI) of the same levels.

Muscle compartments, in life, are encased in a tough fibrous sheath of fascia, facilitating friction-free movement and holding the muscle's characteristic shape [26]. Although the THUMS model's compartments are covered in a shell element layer, this is assigned no significant material properties and is not typical of the fascia. There is no allowance for adipose tissue at any level. The right-hand MRI scans (Figure 5) highlight that there may be a significant quantity of fat to provide potential cushioning to impact [27], particularly at the thigh level. Additional vital structures such as blood vessels and nerves

appear absent from the THUMS model. While they may not convey any biomechanical influence to the tissues, they are of high clinical importance. For example, damage to an artery significantly increases the severity of the injury and may result in an unsalvagable limb.

The homogeneity of lower limb soft tissues was also an approach initially adopted by the Lower Limb Model for Safety (LLMS) [28] which used identical material properties for skin and 'flesh' layers in their model. This was quickly updated to include a separate 'muscle-flesh' layer with evidence-based mechanical properties [29]. Similarly, in the lower limb section of the Global Human Body Model Consortium (GHBMC), Untaroiu et al. differentiate between the skin and 'flesh' through differing material properties but allow for no further detail in these layers [30]. Soft tissue modelling is notoriously difficult, and there are currently no human body models that contain detailed representations of these tissues for impact studies. Perhaps one of the most significant difficulties in modelling these tissues is the considerable variation in evidence around their properties, often based on small samples' mechanical testing. Nonetheless, models of muscle [31], skin [32; 33] and adipose tissue [34] have been proposed in isolation. Incorporating these modelling techniques into a human body model may represent a viable option to improve soft tissue modelling accuracy.

The influence of other soft tissues structures in the lower limb is controversial. The THUMS model contains no specific joint capsule surrounding the knee, and only tissue modelled as 'flesh' spans the knee in place of the many ligaments and tendons present in real life. The presence of a joint capsule and peripheral soft tissues has been shown to influence relaxed knees' stability [35], although their influence on joint mechanics subject to large impact forces has yet to be defined. Interestingly, Beillas et al. included a knee capsule in their LLMS model, assigned similar material properties to the collateral ligaments [28]. The authors do not comment on the effect of the capsule on their knee model's mechanical behaviour.

4 Material Properties

The material properties assigned to selected soft tissues of the THUMS lower leg model are summarised in Table 1. The bones in the THUMS model are composed of two layers representing hard cortical bone surrounding a spongy core of cancellous bone; both are modelled with solid elements. The mechanical properties of these layers are taken from experimental data reported by Yamada et al. [36], comparable to other contemporary models. Cortical bone displays strain rate effects; specifically, its properties (elastic modulus, yield stress and strain) increase with an increasing strain rate [37; 38]. The MAT_024: PIECEWISE_LINEAR_PLASTICITY card allows for the stress-strain curve to be defined at different strain rates. Intriguingly, the properties of bone appear to change significantly during tension, becoming more brittle at increased strain rates [37]. Asgharpour et al. performed a detailed analysis of a femur taken from the THUMS model and compared this with their cadaveric experiments to assess the strain rate dependence. Using the MAT_124: PLASTICITY_COMPRESSION_TENSION card, they could replicate the difference in tension and compression properties and show good agreement with experimental data [39]. This would, therefore, represent a reasonable update to the bony properties in the THUMS model.

Both ligaments and 'flesh' are modelled as solid elements using the MAT_181: SIMPLIFIED_RUBBER card, representing a rubber and foam model response with a single uniaxial load curve. The tissue properties used appear to be evidence-based; however, it is surprising that the quadriceps tendon and ligaments are assigned the same material characteristics. In life, the quadriceps tendon is a thick and robust structure capable of transferring vast forces across the knee joint; the ligaments, on the other hand, are far more delicate and elastic in nature. This may affect their performance during impact, and the following section highlights some of these differences in shear testing.

	Part	Element	Properties	ρ (ton/mm³)	E (N/mm²)	ν
BONE	Femur cortex	Solid	MAT_024: PIECEWISE_LINEAR_PLASTICITY	2.00E-09	17300	0.30
	Femur cancellous	Solid	MAT_105: DAMAGE_2	8.62E-10	40	0.45
	Tibia cortex	Solid	MAT_024: PIECEWISE_LINEAR_PLASTICITY	2.00E-09	18000	0.30
	Tibia cancellous	Solid	MAT_105: DAMAGE_2	8.62E-10	40	0.45
	Fibula cortex	Solid	MAT_024: PIECEWISE_LINEAR_PLASTICITY	2.00E-09	18500	0.30
	Fibula cancellous	Solid	MAT_105: DAMAGE_2	8.62E-10	40	0.45
	Part	**Element**	**Properties**	**ρ (ton/mm³)**	**K (N/mm²)**	**ζ**
LIGAMENT / TENDON	LCL	Solid	MAT_181: SIMPLIFIED_RUBBER	1.10E-09	5555.5	0.2
	MCL	Solid	MAT_181: SIMPLIFIED_RUBBER	1.10E-09	5555.5	0.2
	ACL	Solid	MAT_181: SIMPLIFIED_RUBBER	1.10E-09	5555.5	0.2
	PCL	Solid	MAT_181: SIMPLIFIED_RUBBER	1.10E-09	5555.5	0.2
	Quadriceps tendon	Solid	MAT_181: SIMPLIFIED_RUBBER	1.10E-09	5555.5	0.2
	Part	**Element**	**Properties**	**ρ (ton/mm³)**	**E-A (N/mm²)**	**E-B (N/mm²)**
SOFT TISSUES	Thigh skin	Shell	MAT_034: FABRIC	1.10E-09	11	0
	Leg skin	Shell	MAT_034: FABRIC	1.10E-09	11	0
	Part	**Element**	**Properties**	**ρ (ton/mm³)**	**K (N/mm²)**	**ζ**
	Thigh 'tissues'	Solid	MAT_181: SIMPLIFIED_RUBBER	1.05E-09	1000	0.1
	Leg 'tissues'	Solid	MAT_181: SIMPLIFIED_RUBBER	1.05E-09	1000	0.1

Table 1: Summary of the material properties used in the THUMS lower limb model: ρ:density; E:Young's Modulus (E-A and E-B represent two different values of Young's Modulus); ν: Poisson's ratio; K:bulk modulus; ζ:damping co-efficient.

5 Kinematics and failure

5.1 Quasi-static

The THUMS lower limb model has been validated across an assortment of validation tests. The three-point bending tests described by Schreiber et al. have been used to assess the tibia's bending strength under quasi-static conditions [40]. Figure 6 shows sequential images captured from an animation of the THUMS model undergoing this test, plotting the von Mises stresses. Early in the test, a fibula fracture

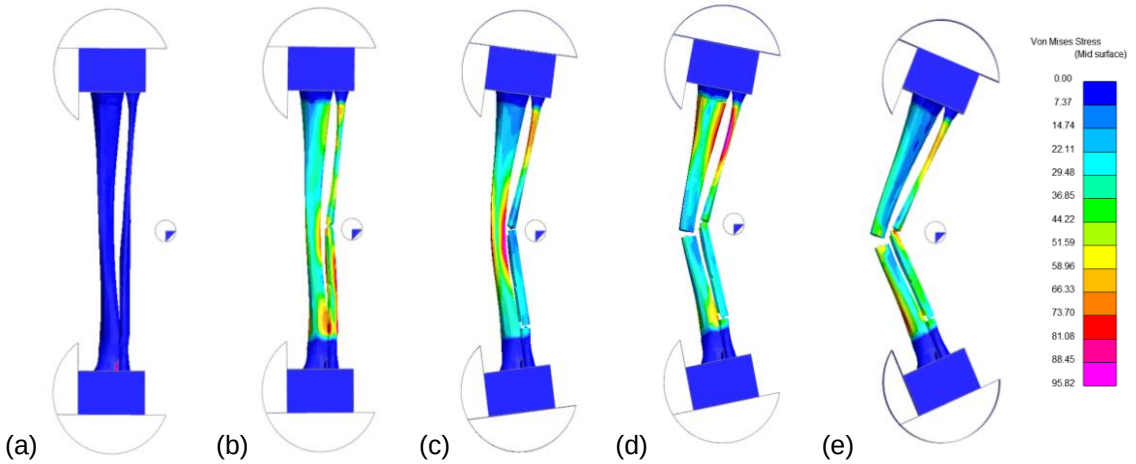

Fig.6: Image sequence taken from tibia 3-point bending testing with contour plot showing von-Mises Stress. Test conditions based on Schrieber et al. [40].

is observed (Fig 6b), followed by a further distal fibula fracture (Fig 6c) and, finally, a diaphyseal tibial fracture (Fig 6d). This bony failure pattern is mainly consistent with the results reported by Schreiber et al., although there is little mention of the nature of fibula fractures in their original paper [40].

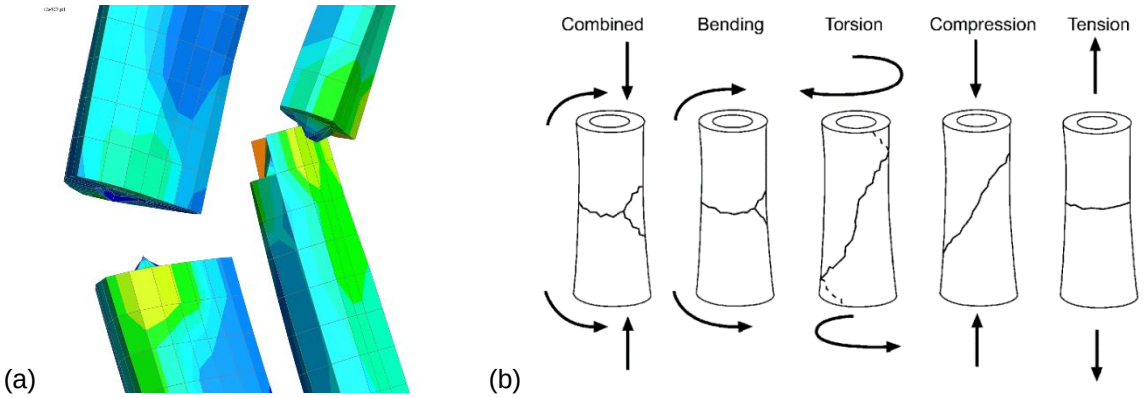

Fig.7: Detailed view of tibia and fibula fractures (a). Common bone fracture patterns according to external load (Reproduced from McGee et al. [42]) (b)

Fractures are simulated in this model using element failure; the material cards for cortical and cancellous bone include a failure strain of 0.0214 and 0.06, respectively. These values for ultimate strain are in agreement with published values [41; 42]. The consequence of element failure appears to be a transverse fracture which is a rather unusual occurrence. Bones often display characteristic fracture patterns according to the type of external load (Figure 7b) [42], and bending forces often cause a transverse fracture at the tension side and a 'butterfly' fragment at the compression side. Comparative assessment of the fracture seen in the THUMS model (Figure 7a) reveals that this compression fragment is absent and hence imprecise in fracture pattern prediction. Accuracy of fracture pattern prediction has been a challenge for contemporary finite element models; whilst the presence or absence of a fracture may be easily predicted, there is often little information about its morphology. There have been several proposed strategies to predict bone crack propagation and therefore fracture pattern. Cohesive finite element modelling has been employed to model bone fracture [43] however is limited as the fracture path must be pre-defined. Element deletion and erosion has been widely used to simulate material failure. This method has been applied to bone fracture [44], where the deleted elements in the mesh determine the fracture pattern. Similarly, element erosion has shown promise in fracture pattern prediction at the whole bone level [45]. Schileo et al. successfully introduced a principal strain-based criteria to model femoral fractures under specific loading conditions [46]. More recently, there has been much interest in extended finite element techniques (XFEM), predicting novel crack propagation between and through elements to generate a fracture pattern [47]. While this is an exciting modelling development, XFEM is not yet widely available and is computationally expensive.

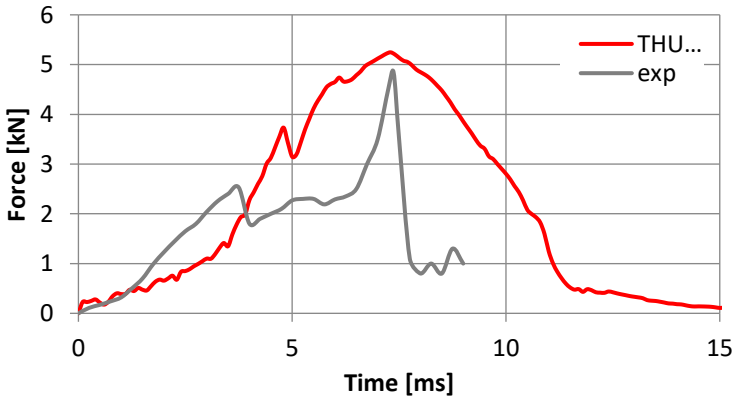

Fig.8: Contact forces between lower leg and impactor (Schreiber et al (grey); THUMS simulation (red)).

There are differences in the shape of the contact force curve simulated by THUMS compared to the experimental data from Schreiber et al. (Figure 8). The sharp peak in the magnitude of the contact force in the cadaver leading up to the fracture point appears as a more gentle curve in THUMS, suggesting an improvement is required in the material definition of the soft tissues or bone in the model.

5.2 Lateral impact

When subjected to a lateral impact at the level of the proximal tibia (based on the experiments conducted by Kajzer et al. [48]), sequential failure of the knee ligaments is observed. The LCL and ACL rupture initially, followed by the PCL later in the simulation (Figure 9). The model's response is in keeping with the injuries reported in the literature in terms of ligaments [48]. Interestingly, ligament failure of the LCL is observed in the mid-substance. In clinical practice, most ligament injuries are observed at the enthesis (ligament-bone interface) [49], making the model's prediction unusual. Further investigation of the ligament model revealed the contact interface to bone was modelled through shared nodes, meaning no failure was permitted at this junction. There has been much work conducted on understanding the complex connection between hard and soft tissue that is observed at the enthesis [50; 51], and attempts have been made to model this structure using finite element techniques [52], however they have yet to be widely adopted into human body models. High principal strain is observed throughout the impact simulation in the distal femur and the proximal tibia; however, both the femoral condyles and tibial plateau regions show no strain. Investigation of the model set-up showed no appreciable difference in the mesh or material characteristics of these regions. Since femoral condyle and tibial plateau fractures [53] are frequently seen during pedestrian trauma, a model must be capable of predicting these injuries.

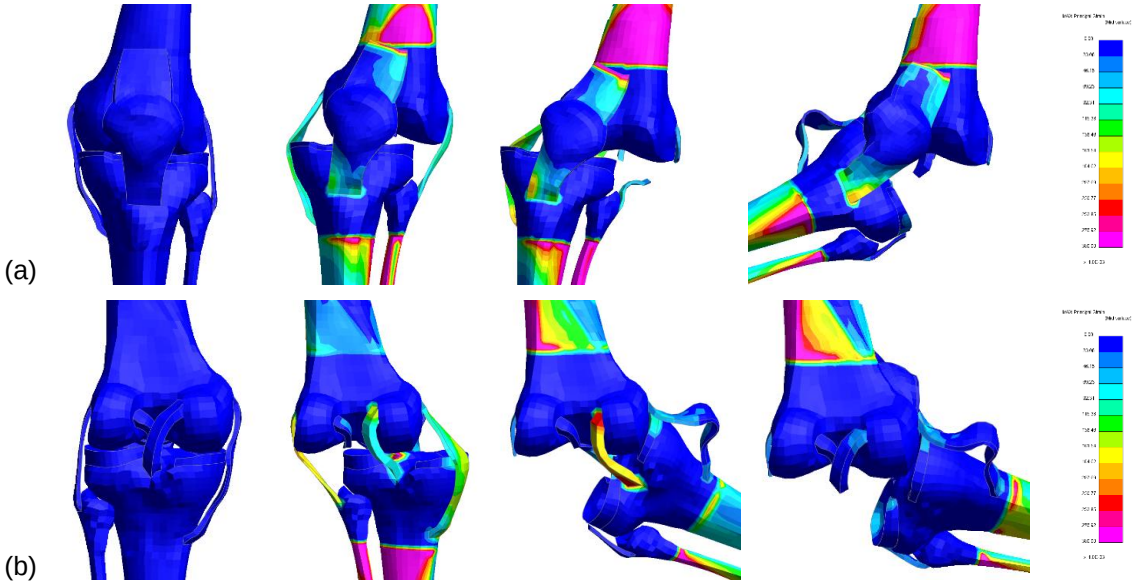

Fig.9: Knee response to lateral impact – (a) anterior view and (b) posterior view. Maximal principal strain plotted with the maximum values set at 30%. Test conditions based on Kajzer et al. [48]

6 Summary

In summary, the THUMS model represents a good attempt at modelling lower limb injuries. Detailed assessment of the geometry has demonstrated excellent agreement with published anthropometric measurements for the skeleton. There is some detail lacking in the ligamentous structures, particularly the cruciate ligaments, although there is currently little evidence suggesting this detail impacts the model's response. The approach taken by the THUMS model for ligament modelling is in keeping with other contemporary human body models. There is concerning simplifications made in the soft tissue mesh, which could be greatly improved with individual muscles and fascial coverings. The inclusion of vessels and nerves could enhance the model's ability to predict severe, limb-threatening injuries and be of great clinical use. Modifying the material models used for ligaments, tendons and 'flesh' could further enhance the model. While assigning material properties to highly elastic, anisotropic biological tissues is challenging; there is evidence that hyperelastic models may provide a more accurate response to impact. The properties applied to bone agree with the current literature; however, simulating failure or fracture is troublesome. The patterns of fractures observed in the experiments described above are unusual and do not reflect those seen in real-life accidents. Currently, there is no straightforward method of modelling crack propagation in bone, although recent advances in extended finite element analysis may prove to enhance fracture pattern prediction. It is crucial to consider the delicate balance between the detail of a model and computational cost; therefore, slight adjustments to this already excellent model may provide the best solution to enhancing our ability to model injury in the lower limb.

7 References

[1] Department for Transport. Reported road casualties in Great Britain: 2019 annual report. *Department for Transport*, *1*, 1 (2019), 36.

[2] Mizuno, Y.; and Ishikawa, H. Summary of IHRA pedestrian safety WG activities-Proposed test methods to evaluate pedestrian protection afforded by passanger cars. In *Proc. 17th Int. Technical Conf. Enhanced Safety of Vehicle*2001, pp. 1–17.

[3] Burgess, A.R.; Dischinger, P.C.; O'Quinn, T.D.; and Schmidhauser, C.B. Lower extremity injuries in drivers of airbag-equipped automobiles: Clinical and crash reconstruction correlations. *Journal of Trauma - Injury, Infection and Critical Care*, *38*, 4 (1995), 509–516.

[4] Shigeta, K.; Kitagawa, Y.; Yasuki, T.; and Corporation, T.M. Development of Next Generation Human FE Model Capable of Organ Injury Prediction. *Proceedings of the 21st ESV Conference*, (2009), 1–20.

[5] Kato, D.; Nakahira, Y.; Atsumi, N.; and Iwamoto, M. Development of human-body model THUMS version 6 containing muscle controllers and application to injury analysis in frontal collision after brake deceleration. *Conference proceedings International Research Council on the Biomechanics of Injury, IRCOBI*, *2018-Septe*, (2018), 207–223.

[6] Maeno, T.; and Hasegawa, J. Development of a Finite Element Model of the Total Human Model for Safety (THUMS) and Application to Car-pedestrian Impacts. In *International Technical Conference on Enhanced Safety of Vehicles*2001.

[7] Wen, L.; Bastien, C.; Blundell, M.; Neal-sturgess, C.; and Kayvantash, K. Stability and Sensitivity of THUMS Pedestrian Model and its Trauma Response to a Real Life Accident. (2015).

[8] Li, G.; Tan, Z.; Lv, X.; and Ren, L. Numerical reconstruction of injuries in a real world minivan-to-pedestrian collision. *Acta of Bioengineering and Biomechanics*, *21*, 2 (2019), 21–30.

[9] Lalwala, M.; Chawla, A.; Thomas, P.; and Mukherjee, S. Finite element reconstruction of real-world pedestrian accidents using THUMS pedestrian model. *International journal of crashworthiness*, *25*, 4 (2020), 360–375.

[10] ARUP. Oasys Suite (Version 17). (2020).

[11] Toyota. THUMS (Pedestrian Version AM 4.02). (2021).

[12] Pan, N. Length of Long Bones and their Proportion to Body Height in Hindus. *Journal of anatomy*, *58*, Pt 4 (1924), 374–8.

[13] Ide, Y.; Matsunaga, S.; Harris, J.; O'Connell, D.; Seikaly, H.; and Wolfaardt, J. Anatomical examination of the fibula: Digital imaging study for osseointegrated implant installation. *Journal of Otolaryngology - Head and Neck Surgery*, *44*, February (2015).

[14] Bokariya, P.; Sontakke, B.; Waghmare, J.E.; Tarnekar, A.; Tirpude, B.H.; and Shende, M.R. The anthropometric measurements of tibia. *Journal of Indian Academy of Forensic Medicine*, *34*, 4 (2012), 322–323.

[15] Grood, E.S.; Noyes, F.R.; Butler, D.L.; and Suntay, W.J. Ligamentous and capsular restraints preventing straight medial and lateral laxity in intact human cadaver knees. *JBJS*, *63*, 8 (1981).

[16] LaPrade, R.F.; Engebretsen, A.H.; Ly, T. V; Johansen, S.; Wentorf, F.A.; and Engebretsen, L. The anatomy of the medial part of the knee. *The Journal of Bone and Joint Surgery. American Volume*, *89*, 9 (2007), 2000–2010.

[17] Memarzadeh, A.; and Melton, J.T.K. Medial collateral ligament of the knee: anatomy, management and surgical techniques for reconstruction. *Orthopaedics and trauma*, *33*, 2 (2019), 91–99.

[18] Liu, F.; Yue, B.; Gadikota, H.R.; Kozanek, M.; Liu, W.; Gill, T.J.; Rubash, H.E.; and Li, G. Morphology of the medial collateral ligament of the knee. *Journal of orthopaedic surgery and research*, *5*, 1 (2010), 69.

[19] Grawe, B.; Schroeder, A.J.; Kakazu, R.; and Messer, M.S. Lateral Collateral Ligament Injury About the Knee: Anatomy, Evaluation, and Management. *JAAOS - Journal of the American Academy of Orthopaedic Surgeons*, *26*, 6 (2018).

[20] Espregueira-Mendes; Vieira Da Silva, M.; and Silva, M.V. Da. Anatomy of the lateral collateral ligament: a cadaver and histological study. *Knee Surgery, Sports Traumatology, Arthroscopy*, *14*, 3 (2005), 221.

[21] Arnoczky, S.P. Anatomy of the Anterior Cruciate Ligament. *Clinical Orthopaedics and Related Research*®, *172*, (1983).

[22] Margheritini, F.; Rihn, J.; Musahl, V.; Mariani, P.P.; and Harner, C. Posterior cruciate ligament injuries in the athlete: an anatomical, biomechanical and clinical review. *Sports medicine (Auckland, N.Z.)*, *32*, 6 (2002), 393–408.

[23] Cone, S.G.; Howe, D.; and Fisher, M.B. Size and Shape of the Human Anterior Cruciate Ligament and the Impact of Sex and Skeletal Growth. *JBJS Reviews*, *7*, 6 (2019), e8.

[24] Harner, C.D.; Xerogeanes, J.W.; Livesay, G.A.; Carlin, G.J.; Smith, B.A.; Kusayama, T.; Kashiwaguchi, S.; and Woo, S.L.Y. The Human Posterior Cruciate Ligament Complex: An Interdisciplinary Study: Ligament Morphology and Biomechanical Evaluation. *The American Journal of Sports Medicine*, *23*, 6 (1995), 736–745.

[25] Woodmass, J.M.; LaPrade, R.F.; Sgaglione, N.A.; Nakamura, N.; and Krych, A.J. Meniscal Repair. *Journal of Bone and Joint Surgery - American Volume*, *99*, 14 (2017), 1222–1231.

[26] Garfin, S.R.; Tipton, C.M.; Mubarak, S.J.; Woo, S.L.; Hargens, A.R.; and Akeson, W.H. Role of fascia in maintenance of muscle tension and pressure. *Journal of Applied Physiology Respiratory Environmental and Exercise Physiology*, *51*, 2 (1981), 317–320.

[27] Arbabi, S.; Wahl, W.L.; Hemmila, M.R.; Kohoyda-Inglis, C.; Taheri, P.A.; and Wang, S.C. The Cushion

Effect. *Journal of Trauma and Acute Care Surgery*, *54*, 6 (2003).
[28] Beillas, P.; Begeman, P.C.; Yang, K.H.; King, A.I.; Arnoux, P.-J.J.; Kang, H.-S.S.; Kayvantash, K.; Brunet, C.; Cavallero, C.; and Prasad, P. Lower Limb: Advanced FE Model and New Experimental Data. In *Stapp Car Crash Journal*2001.
[29] Behr, M.; Arnoux, P.J.; Serre, T.; Bidal, S.; Kang, H.S.; Thollon, L.; Cavallero, C.; Kayvantash, K.; and Brunet, C. A human model for road safety: from geometrical acquisition to model validation with radioss. *Computer methods in biomechanics and biomedical engineering*, *6*, 4 (2003), 263–273.
[30] Untaroiu, C.; Darvish, K.; Crandall, J.; Deng, B.; and Wang, J.-T. A Finite Element Model of the Lower Limb for Simulating Pedestrian Impacts. *Stapp Car Crash Journal*, *49*, (2005), 157–81.
[31] Xiang, Y.; and Arefeen, A. Computational Methods for Skeletal Muscle Strain Injury: A Review. *Critical reviews in biomedical engineering*, *47*, 4 (2019), 277–294.
[32] Soetens, J.F.J.J.; van Vijven, M.; Bader, D.L.; Peters, G.W.M.M.; and Oomens, C.W.J.J. A model of human skin under large amplitude oscillatory shear. *Journal of the mechanical behavior of biomedical materials*, *86*, July (2018), 423–432.
[33] Bischoff, J.E.; Arruda, E.M.; and Grosh, K. Finite element modeling of human skin using an isotropic, nonlinear elastic constitutive model. *Journal of biomechanics*, *33*, 6 (2000), 645–652.
[34] Gepner, B.; Joodaki, H.; Sun, Z.; Jayathirtha, M.; Kim, T.; and Kerrigan, J. Performance of the Obese GHBMC Models in the Sled and Belt Pull Test Conditions. *ICROBI Conference 2018*, (2018).
[35] Naghibi Beidokhti, H.; Janssen, D.; van de Groes, S.; Hazrati, J.; Van den Boogaard, T.; and Verdonschot, N. The influence of ligament modelling strategies on the predictive capability of finite element models of the human knee joint. *Journal of Biomechanics*, *65*, (2017), 1–11.
[36] Yamada, H.; and Evans, F.G. *Strength of biological materials*. Baltimore, Md: Williams & Wilkins, 1970.
[37] Hansen, U.; Zioupos, P.; Simpson, R.; Currey, J.D.; and Hynd, D. The Effect of Strain Rate on the Mechanical Properties of Human Cortical Bone. *Journal of biomechanical engineering*, *130*, 1 (2008), 11011.
[38] McElhaney, J.H. Dynamic response of bone and muscle tissue. *Journal of applied physiology*, *21*, 4 (1966), 1231–1236.
[39] Asgharpour, Z.; Zioupos, P.; Graw, M.; and Peldschus, S. Development of a strain rate dependent material model of human cortical bone for computer-aided reconstruction of injury mechanisms. *Forensic science international*, *236*, C (2014), 109–116.
[40] Schreiber, P.; Crandall, J.; Hunvitz, S.; and Nusholtz, G.S. Static and dynamic bending strength of the leg. *International Journal of Crashworthiness*, *3*, 3 (1998), 295–308.
[41] Wolfram, U.; and Schwiedrzik, J. Post-yield and failure properties of cortical bone. *BoneKEy Reports*, *5*, (2016), 829.
[42] McGee, A.M.; Qureshi, A.A.; and Porter, K.M. Review of the biomechanics and patterns of limb fractures. *Trauma (London, England)*, *6*, 1 (2004), 29–40.
[43] Ural, A.; Zioupos, P.; Buchanan, D.; and Vashishth, D. The effect of strain rate on fracture toughness of human cortical bone: A finite element study. *Journal of the mechanical behavior of biomedical materials*, *4*, 7 (2011), 1021–1032.
[44] Ridha, H.; and Thurner, P.J. Finite element prediction with experimental validation of damage distribution in single trabeculae during three-point bending tests. *Journal of the Mechanical Behavior of Biomedical Materials*, *27*, (2013), 94–106.
[45] Niebur, G.L.; Feldstein, M.J.; Yuen, J.C.; Chen, T.J.; and Keaveny, T.M. High-resolution "nite element models with tissue strength asymmetry accurately predict failure of trabecular bone. *Journal of Biomechanics*, *33*, (2000), 1575.
[46] Schileo, E.; Taddei, F.; Cristofolini, L.; and Viceconti, M. Subject-specific finite element models implementing a maximum principal strain criterion are able to estimate failure risk and fracture location on human femurs tested in vitro. *Journal of biomechanics*, *41*, 2 (2007), 356–367.
[47] Ali, A.A.; Cristofolini, L.; Schileo, E.; Hu, H.; Taddei, F.; Kim, R.H.; Rullkoetter, P.J.; and Laz, P.J. Specimen-specific modeling of hip fracture pattern and repair. *Journal of biomechanics*, *47*, 2 (2013), 536–543.
[48] Kajzer, J.; Schroeder, G.; Ishikawa, H.; Matsui, Y.; and Bosch, U. Shearing and Bending Effects at the Knee Joint at High Speed Lateral Loading. *SAE transactions*, *106*, (1997), 3682–3696.
[49] Gardiner, J.C.; Weiss, J.A.; and Rosenberg, T.D. Strain in the human medial collateral ligament during valgus loading of the knee. In *Clinical Orthopaedics and Related Research*2001, pp. 266–274.
[50] Tits, A.; and Ruffoni, D. Joining soft tissues to bone: Insights from modeling and simulations. *Bone Reports*, *14*, July 2020 (2021), 100742.
[51] Subit, D.; Masson, C.; Brunet, C.; and Chabrand, P. Microstructure of the ligament-to-bone attachment complex in the human knee joint. *Journal of the mechanical behavior of biomedical materials*, *1*, 4 (2008), 360–367.
[52] Thomopoulos, S.; Marquez, J.P.; Weinberger, B.; Birman, V.; and Genin, G.M. Collagen fiber orientation at the tendon to bone insertion and its influence on stress concentrations. *Journal of Biomechanics*, *39*, 10 (2006), 1842–1851.
[53] Otte, D.; and Haasper, C. Characteristics on fractures of tibia and fibula in car impacts to pedestrians and bicyclists - influences of car bumper height and shape. *Annual proceedings - Association for the Advancement of Automotive Medicine*, *51*, (2007), 63–79.